Electronic Supporting Information (ESI)

N-doped hierarchical porous carbon prepared by simultaneous-activation of KOH and NH3 for high performance supercapacitor

Nannan Guo,[a] Min Li,[a] Yong Wang,[ab] Xingkai Sun,[a] Feng Wang*[a] and Ru Yang*[a]

[a] *State Key Laboratory of Chemical Resource Engineering, Beijing Key Laboratory of Electrochemical Process and Technology for Materials, Beijing University of Chemical Technology, Beijing 100029 China*

[b] *North Institute for Scientific & Technical Information, Beijing 100089 China*

Corresponding authors. Tel: +86 10 64436736; E-mail: ruyang@mail.buct.edu.cn (R. Yang).

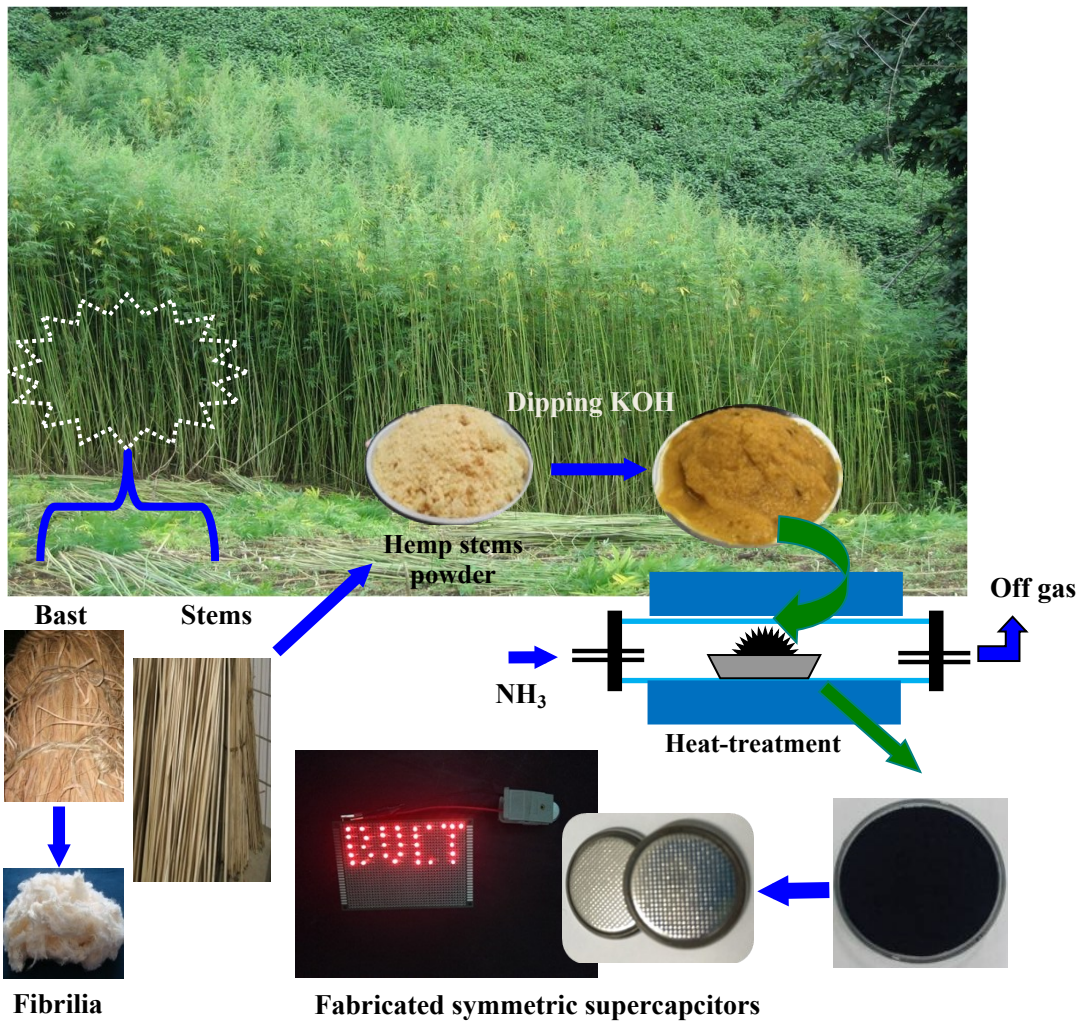

Fig. S1 Schematic illustration of nitrogen doping porous carbons prepared by KOH activation under NH_3 flow from hemp stems.

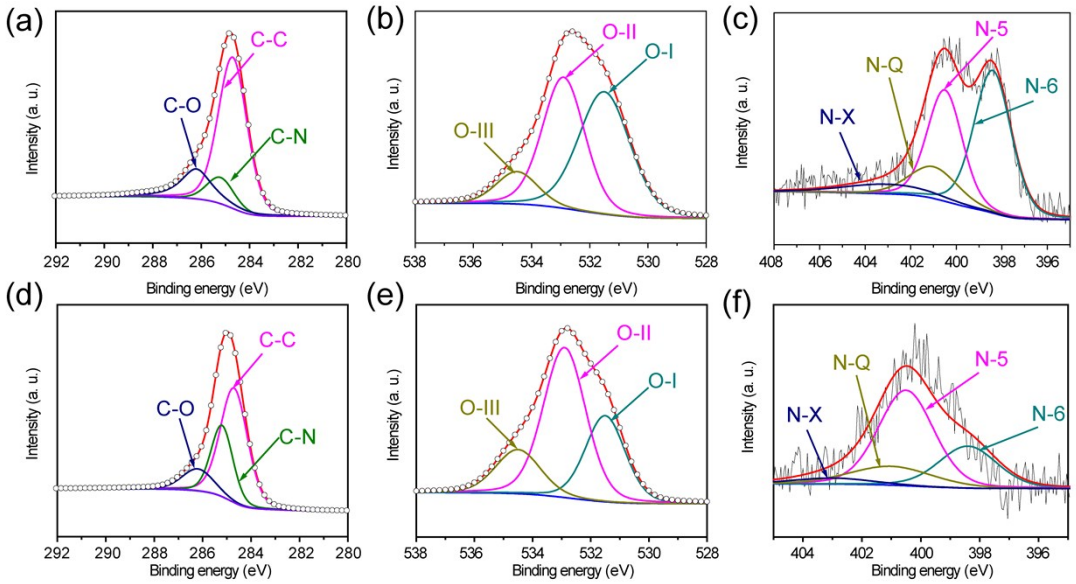

Fig. S2 High-resolution XPS spectra: (a) C1s, (b) O1s, (c) N1s of APC-750; (d) C1s, (e) O1s, (f) N1s of KPC-750.

Table. S1 Surface elementary composition and contents of different kinds of N, O of the AKPC-750, KPC-750 and APC-750

Sample	N	O	N-6	N-5	N-Q	N-X	O-I	O-II	O-III
	(at.%)	(at.%)	(at.%)	(at.%)	(at.%)	(at.%)	(at.%)	(at.%)	(at.%)
AKPC-750	4.2	8.8	1.79	1.46	0.53	0.42	3.98	3.73	1.09
APC-750	2.8	11	1.28	0.94	0.37	0.2	5.25	4.63	1.12
KPC-750	1.7	8	0.43	0.92	0.27	0.08	2.33	4.33	1.34

AKPC-750

KPC-750

APC-750

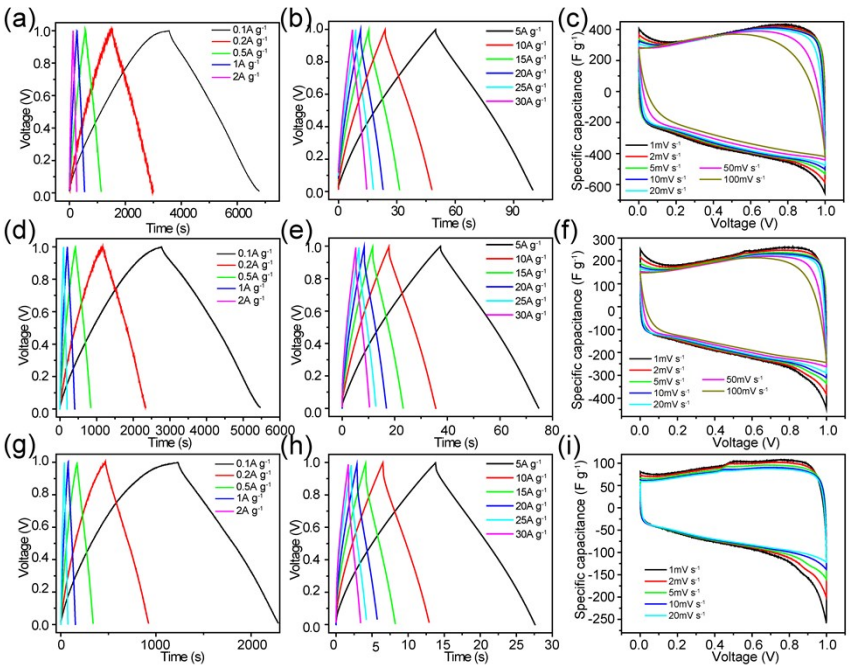

Fig. S3 (a), (b), (d), (e), (g) and (h) Galvanostatic charge-discharge curves at different current density; (c), (f), (i) cyclic voltammetry curves at different scan rate in a three-electrode system with 6 M KOH as electrolyte.

AKPC-750

KPC-750

APC-750

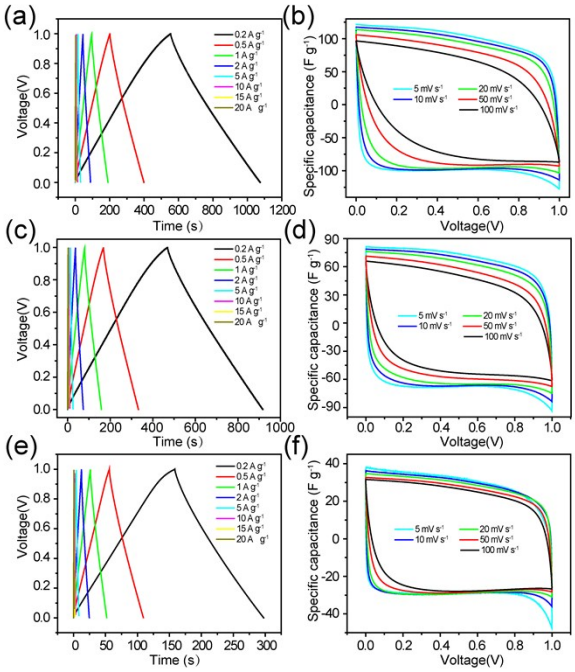

Fig. S4 (a), (c) and (e) Galvanostatic charge discharge curves at different current density; (b), (d) and (f) Cyclic voltammetry curves at different scan rate in a two-electrode system with 6 M KOH as electrolyte.

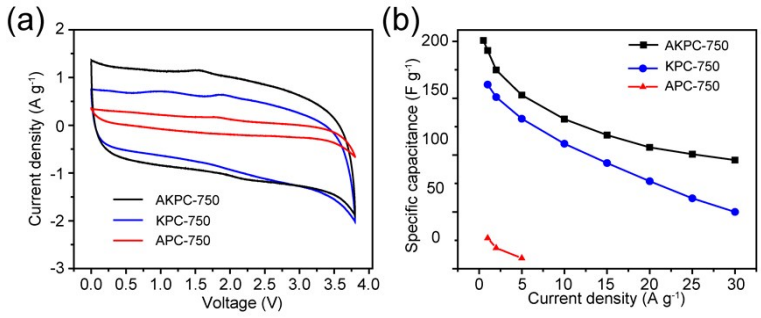

Fig. S5 (a) Cyclic voltammetry curves at 10mV s^{-1}; (b) Specific capacitance of AKPC-750, KPC-750 and APC-750 based symmetrical supercapacitors at different current densities in neat EMIM TFSI.

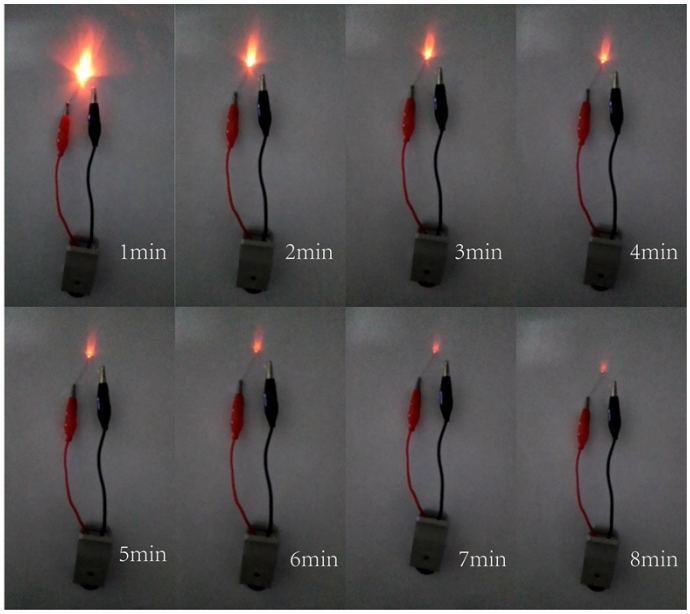

Fig. S6 Photograph of a red LED lit by AKPC-750 based supercapacitor in ionic liquid.

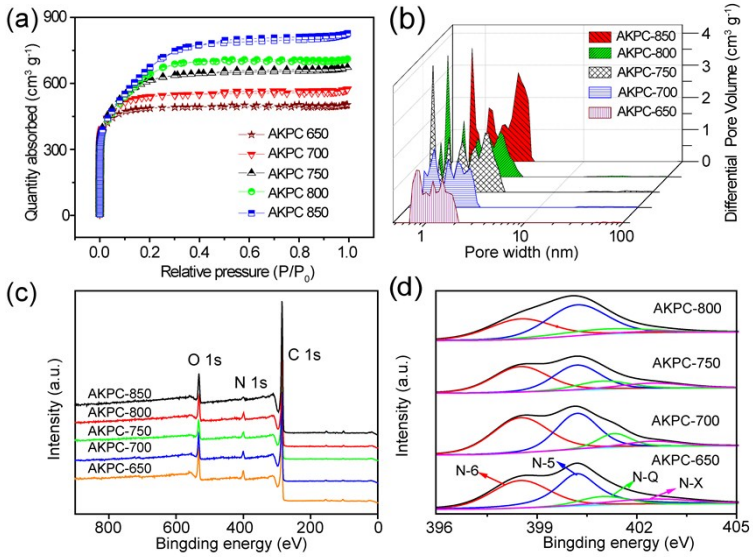

Fig. S7 Nitrogen adsorption-desorption isotherms at -196 ºC; (b) DFT pore size distributions; (c) XPS survey spectra and (d) high resolution N 1s XPS spectra of AKPCs.

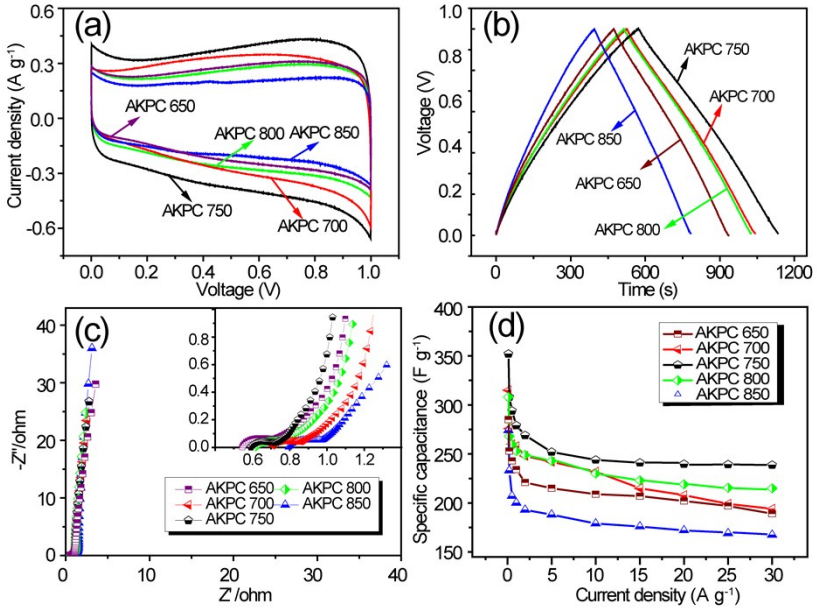

Fig. S8 (a) Cyclic voltammetry curves at 1 mV s^{-1}; (b) Galvanostatic charge discharge lines obtained at 0.5 A g^{-1}; (c) Nyquist plot and the inset reveals the magnified high-frequency region of the plot; (d) Specific capacitance at different current densities for AKPCs based electrodes in 6 M KOH in three-electrode system.

Table S2. Textual parameters deduced from N_2 adsorption- desorption at -196 °C and elementary composition evaluated from elemental analysis of the AKPCs.

Sample	$^{a}S_{BET}$	$^{b}V_{total}$	$^{c}V_{micro}$	$^{d}V_{meso}$	N	C	O
	(m^2 g^{-1})	(m^3 g^{-1})	(cm^3 g^{-1})	(cm^3 g^{-1})	(wt.%)	(wt.%)	(wt.%)
AKPC-650	1486	0.51	0.48	0.02	5.3	60.7	31.3
AKPC-700	1659	0.63	0.58	0.03	4.7	69.6	24.4
AKPC-750	1949	0.88	0.68	0.18	4.4	75.8	17.9
AKPC-800	2111	0.96	0.59	0.33	3.3	83.7	11.6
AKPC-850	2331	1.10	0.51	0.52	1.7	85.3	11.9

a: The specific surface area; b: Total pore volume obtained by DFT; c: Micropore volume calculated by DFT; d: Mesopore volume calculated by DFT.

In order to further confirm the key role of the high specific surface area, hierarchical pore size distribution and high nitrogen oxygen and content in the electrochemical applications, a series of control sample heated at different temperature under NH_3 were prepared. Fig.S7a shows the nitrogen adsorption-desorption isotherms of AKPCs prepared at different temperatures. All samples display type I nitrogen adsorption isotherms. Major adsorption of the samples occurs at a low relative pressure of less than 0.1 and gives rise to an almost horizontal plateau at higher relative pressure, indicating high microporosity in samples. With the increase of heating temperature, the evidently increased adsorption volume indicates more developed pore structure, wider knee at lower relative pressure indicates wider pores, proving that temperature plays important parameter for tailoring the development of porosity in activation process. Furthermore, the pore size distribution curves (Fig.S7b) provide an apparent evidence for hierarchical pore structure with ultramicropores (<1 nm), micropores (1-2 nm) and mesopores (2-4 nm) and the pore size becoming larger with the increase of reaction temperature. The pore texture parameters changing with temperature are shown in Table.S1. The BET specific surface area of the samples increase dramatically from 1486 to 2331 m^2 g^{-1} when temperature rises from 650°C to 850°C. However, with the increasing of temperature from 650 to 850 °C, the carbon content increases continuously from 60.7 to 85.3 wt.%, while the heteroatoms decrease obviously (O: 31.3-11.9 and N: 5.3-1.7 wt.%). Although decreasing with the activation temperature, the nitrogen content still contains a high level when the temperature below 850 °C. X-ray photoelectron spectroscopy (XPS) measurements were conducted to elucidate the surface chemical compositions and the nitrogen configurations of the AKPCs (Fig.S7c and d).

To evaluate the electrochemical performance of the as-synthesized samples as supercapacitor electrodes, cyclic voltammetry (CV) and galvanostatic charge-discharge (GCD) measurements were calculated in 6 M KOH aqueous electrolyte using a three electrode system. It is interesting that the specific capacitance of AKPC-750 in both CV and GCD curves is higher than those for other samples. We ascribe this to the balance of specific surface area and nitrogen content. Although the nitrogen content of AKPC-750 (4.4 wt.%) is lower than that of AKPC-650 (5.3 wt.%) and AKPC-700 (4.7 wt.%), the specific surface area of AKPC-750 (1949 $m^2 g^{-1}$) is much higher than that of AKPC-650 (1486 $m^2 g^{-1}$) and AKPC-700 (1659 $m^2 g^{-1}$). Although the specific surface area of AKPC-850 (2331 $m^2 g^{-1}$) and AKPC-800 (2111 $m^2 g^{-1}$) are slightly higher than that of AKPC-750 (1949 $m^2 g^{-1}$), the nitrogen content of AKPC-750 (4.4 wt.%) is higher than AKPC-850 (1.7 wt.%) and AKPC-800 (3.3 wt.%), as listed in Tables.S1. The co-contribution of the high electronic double-layer capacitance due to its high surface area and the additional pseudocapacitance mainly derived from the doped nitrogen endows AKPC-750 with the largest specific capacitance of 352 F g^{-1} at 0.1 A g^{-1}, higher than those of AKPC-650 (285 F g^{-1}), AKPC-700 (315 F g^{-1}), AKPC-800 (308 F g^{-1}), AKPC-850 (274 F g^{-1}). Based on the above results, we known that a combination of high specific surface area, proper porous structure and favorable nitrogen- and oxygen-doping synergistically leads to the extraordinary electrochemical performance.